Effect of scattering on nonlinear optical scanning microscopy imaging of highly scattering media

Jinpin Ying, Feng Liu, and R. R. Alfano

The intensity of two-photon excited fluorescence (TPF) generated by ultrashort laser pulses was measured as a function of the depth of a focal point inside highly scattering media. The purpose was to investigate the spatial location of TPF in a scattering medium. Owing to the scattering, the intensity of the incident beam as well as the generated TPF signal was attenuated exponentially as the focal point was scanned into the medium. As the scattering strength of the medium was increased, the TPF was not confined to the focal region and had a wider distribution. These observations show that the scattering will result in the degradation of the ability of optical depth sectioning of nonlinear optical scanning microscopy. © 2000 Optical Society of America

OCIS codes: 190.4180, 290.7050, 180.0180, 110.6880, 180.1790.

1. Introduction

Nonlinear optical scanning microscopy has been widely used to obtain three-dimensional (3-D) imaging of the microstructures of various materials.[1–6] With this technique, nonlinear optical signals, such as two-photon excited fluorescence (TPF) and second harmonic generation are generated when a laser beam is focused into a sample by using a microscope objective lens. By scanning the focal point inside the sample, one detects nonlinear optical signals reemitted from the sample surface in the backward or forward direction to obtain a 3-D image of optical properties of the sample. Owing to the nonlinear dependence of a signal, for example, the quadratic dependence of two-photon fluorescence on the excitation intensity, the nonlinear optical signal is confined mainly to the focal region of the incident beam for a weakly scattering medium.[7] When a microscope objective lens with a high numerical aperture is used, the focal spot region could be small (a volume of 0.4 μm in diameter by 1.2 μm in length). Thus the nonlinear optical signal directly reflects the local optical properties of the focal region. This allows nonlinear optical scanning microscopy to obtain a 3-D image of the sample structure with a very spatial high resolution (0.5 μm).

Two-photon fluorescence (TPF) uses two photons to excite the material, allowing one to obtain fluorescence emission at shorter wavelengths than the excitation wavelength. There are many important native fluorophors in biological systems that can be probed by TPF, such as tryptophan, elastin, collagen, and nicotinamide adenine dinucleotide (NADH). The excitation band resides in the UV and visible regions.[8,9] However, UV radiation is a potential hazard to tissues. Hence the TPF process eliminates the necessity of using direct UV radiation. For imaging tissue structure, the TPF technique can image deeper into a sample than single-photon excitation because of reduced scattering in tissues at longer wavelengths.[10]

For nonscattering or weakly scattering media, because of the quadratic dependence of two-photon fluorescence on the excitation intensity, the TPF signal originates mainly from the focal volume. The other parts of the sample are immersed in a photon cone of near-IR excitation and do not contribute much to the emitted signal.[1,8] The TPF signal directly reflects optical properties at the focal volume. This fact allows a large-area photodetector to image the media that is useful especially when fluorescence intensity is weak.[1,8] However, for highly scattering media ($\mu_s > 1.0\ mm^{-1}$), such as biological tissues, the intensity of the excitation light is attenuated as the light travels into the medium. It was found that TPF is

The authors are with the Department of Physics, Institute for Ultrafast Spectroscopy and Lasers, New York State Center for Advanced Technology for Ultrafast Photonic Materials and Applications, The City College and the Graduate School of the City University of New York, New York, New York 10031.

Received 27 May 1999; revised manuscript received 5 October 1999.

0003-6935/00/040509-06$15.00/0

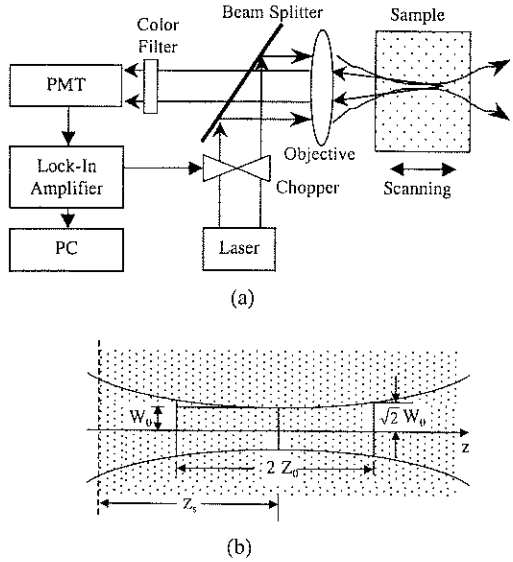

Fig. 1. (a) Schematic diagram of the experimental setup. (b) Schematic of beam propagation geometry. The beam is incident from the left, and w_0 is the beam waist.

not well confined to the focal region when the focal spot is more than five scattering mean free paths (MFP's) inside the medium.[7] The TPF intensity at the focal region is significantly reduced compared with the one generated closer to the sample surface.[7] Our experimental observation qualitatively agrees with the recent theoretical research of Blanca and Saloma[11] using Monte Carlo simulation. The theoretical model for the scattering effect on the generation of a nonlinear signal was also investigated in our previous paper.[7] When the scattering of the medium is taken into account, our model qualitatively explains the observed spatial distribution of the nonlinear optical signal.

TPF reemitted from different regions inside a scattering sample experiences a different amount of scattering. The TPF signals from sections located deep in the surface of the medium will experience more scattering than ones closer to the surface. Thus the confinement of TPF to the focal region is degraded as the scattering of the medium increases. In this case, scattering results in the degradation of the optical depth sectioning ability and the resolution of two-photon fluorescence microscopy.

The purpose of this study is to investigate the effect of scattering on both the generation and the reemission strength of TPF in highly scattering media. TPF signals from uniform scattering media having different scattering strengths are measured as a function of focal depth. A theoretical model describing the spatial TPF intensity distribution from scattering media is presented and compared with the experimental results.

2. Experimental Methods and Materials

The experimental arrangement is shown schematically in Fig. 1(a). It is similar to a scanning microscope in backscattering geometry. A Ti:Sapphire laser system (Mira 900f, Coherent Laser Corporation) was used to generate laser pulses of 120-fs duration at a 810-nm central wavelength. The repetition rate of the laser pulses was 76 MHz. The TPF signal was generated by focusing a laser pulse reflected from a dichroic beam splitter into a scattering media by using a microscope objective lens (20×, N.A. = 0.4). The backscattered TPF light from the sample was collected by the same objective lens and transmitted through the dichroic beam splitter to a photomultiplier tube (PMT) (Model R928, Hamamatsu) for detection. A computer-controlled lock-in amplifier (Model SR512, Stanford) was used to detect and record the electronic signal from the PMT. Two short bandpass filters (BG-39, CVI) were placed in front of the PMT to block the excitation light. The TPF intensity profile was detected as the focal point was scanned in and out of the medium by a motorized translation stage. The incident power of the Gaussian beam on the sample surface was less than 10 mW.

The active scattering sample medium, placed in a square glass cell, was a mixture of Rhodamine 590 Tetrafluoroborate dye (Exciton) in a scattering host media consisting of a polystyrene sphere suspension (Duke Scientific Corporation) in methanol. The dimension of the square glass cell was approximately 1.5 cm × 2.5 cm × 3 cm. The path length of the excitation light in the cell was ~1.5 cm. The concentration of the dye was 1.9×10^{-4} M/liter. The emission band was centered around 550 nm with a bandwidth of 40-nm FWHM. The absorption coefficient of the dye at a 550-nm wavelength was 0.76 mm^{-1} and was less than 0.01 mm^{-1} at a 810-nm wavelength when the transmission through the neat dye was measured with a spectrometer (Model Lambda9, Perkin Elmer). Adding various amounts of 10% polystyrene sphere scatterer into the dye solution changed the scattering strength of the media. Polystyrene spheres with diameter sizes of 0.304 and 1.07 μm were used as scattering media to investigate the effect of the scattering function on the TPF signal. The concentration and scattering parameters of two sets of samples are listed in Table 1. The scattering parameters were computed by Mie theory.[12] The indices of refraction were 1.59 and 1.33 for polystyrene and methanol, respectively. For a smaller-size scatterer of 0.304 μm, the asymmetric scattering parameter g (mean cosine of the scattering angle) was 0.45 at a 810-nm and 0.72 at a 550-nm emission band. The g factor for a larger-size (1.07-μm) scatterer was 0.90 and 0.92 at 810 and 550 nm, respectively. The asymmetric parameter for a scatterer of 1.07-μm size was similar to values for tissues in the visible and the near-IR spectral region.[10] The scattering function (differential scattering cross section) of the smaller particle is more isotropic than the large scatterer. For larger scatterers, the light wave is mostly scattered in the forward direction.

Table 1. Comparison of the Theoretical Decay Slope of the TPF Profile with Experimental Results for Two Kinds of Scattering Media

Volume Concentration of Scatterer (%)	μ_s (mm^{-1})		Decay Slope of TPF (mm^{-1})	
	550 nm	810 nm	Experiment	Theory
	Media 1 (Diameter, 0.304 μm)			
0.13	2.11	0.78	3.9	3.9
0.26	4.18	1.57	6.0	7.3
0.38	6.13	2.32	7.3	10.2
0.51	8.17	3.07	9.1	12.4
0.63	10.1	3.77	10.3	14.0
	Media 2 (Diameter, 1.07 μm)			
0.025	1.08	0.63	1.9	2.7
0.033	1.44	0.83	2.1	3.4
0.05	2.16	1.25	3.1	4.9
0.1	4.33	2.50	5.1	8.9
0.2	8.65	5.00	7.6	14.4

3. Theoretical Model

The beam propagation geometry is shown in Fig. 1(b). The medium can be considered semi-infinite. The detected backscattered TPF signal can be viewed as the result of a two-step process: (1) A 3-D distribution of TPF was generated by a focused Gaussian laser beam attenuated by scattering. (2) The generated TPF propagated out of the scattering medium and was detected by the objective lens. The detected TPF is a convolution of these two steps and can be written as

$$I_{tpf} \propto \int I_g(\mathbf{r}')G_{em}(\mathbf{r}, \mathbf{r}')\, d^3r', \tag{1}$$

where $I_g(\mathbf{r}')$ is the nonlinear optical signal generated by the excitation beam and $I_g(\mathbf{r}') = c(\mathbf{r}')I_{ex}{}^2(\mathbf{r}')$ for the TPF signal. $I_{ex}(\mathbf{r}')$ is the excitation intensity at $\mathbf{r}'$, and $c(\mathbf{r}')$ is the local fluorophor concentration. $G_{em}(\mathrm{r}, \mathrm{r}')$ is the propagation Green's function for nonlinear optical light propagating out of the medium. For typical microscopy imaging of tissues, the depth penetration is as many as 10 scattering MFP's (~1 mm).

In this paper, theoretical modeling as a first-order approximation is used and the effect of scattering on light propagation is represented as attenuation loss. The ballistic or coherent component is considered, and the diffuse component is neglected in our computation.

In the first-order approximation, the Gaussian excitation beam is ballistic, attenuated exponentially according to the Beer–Lambert law. For a uniform scattering medium, the intensity profile of a focused Gaussian laser beam with focal point at z_s inside the medium at position (ρ, z) can be described by[7,13]

$$I_{ex}(\rho, z) = I_0\left[\frac{w_0}{w(z)}\right]^2 \exp\left[-\frac{2\rho^2}{w^2(z)}\right] \exp(-\mu_s{}^{ex}z), \tag{2}$$

where $w_0 = (\lambda z_0/\pi)^{1/2}$ is the beam waist, $w(z) = w_0\{1 + [(z - z_s)/z_0]^2\}^{1/2}$, ρ is the radial coordinates, I_0 is the peak intensity of the Gaussian beam at $z = z_s$, $\mu_s{}^{ex}$ is the scattering coefficient of the medium at the excitation (810 nm), $\mu_s{}^{ex} \gg \mu_a{}^{ex}$, where $\mu_a{}^{ex}$ is the absorption coefficient of the medium at the excitation (810 nm). The surface of the media was set at $z = 0$ in these coordinates, and z_0 is the depth of focus (the confocal parameter).

The 3-D TPF generated by the focused Gaussian beam can be written as

$$I_g(\rho, z) \propto I_{ex}{}^2(\rho, z) = I_0{}^2\left[\frac{w_0}{w(z)}\right]^4 \exp\left[-\frac{4\rho^2}{w^2(z)}\right] \exp(-2\mu_s{}^{ex}z). \tag{3}$$

The active dye molecules in our experiment were distributed uniformly in the sample, $c(\mathbf{r}')$ = constant. In the approximation the reemission process is described by ballistic transport. For a uniform medium $G_{em}(\mathbf{r}, \mathbf{r}')$, Green's function of ballistic propagation for light reemitted back from the medium along the z axis is

$$G_{em}(\mathbf{r}, \mathbf{r}') = \exp[-(\mu_s{}^{em} + \mu_a{}^{em})|z - z'|], \tag{4}$$

where $\mu_s{}^{em}$ and $\mu_a{}^{em}$ are the scattering and the absorption coefficients, respectively, of the medium at the emission wavelength (550 nm).

After integration over the lateral dimension is performed, the detected TPF as a function of focal depth z_s can be written as

$$I_{tpf}(z_s) \propto \int_0^\infty 1/[1 + (z - z_s)^2/z_0{}^2] \times \exp[-(2\mu_s{}^{ex} + \mu_s{}^{em} + \mu_a{}^{em})z]\, dz. \tag{5}$$

The first factor in Eq. (5) describes the axial confinement of the focused Gaussian beam at the focal position z_s. The exponential factor describes the scattering and the absorption loss of both excitation and reemitted TPF light. The factor of 2 for the scattering coefficient of excitation reflects the quadratic intensity dependence of TPF on the excitation light intensity.

As described in Section 2, when a motorized translation stage scans the focal point of the laser beam in the medium, the TPF intensity profile can be detected as a function of the focal position z_s. From Eq. (5) theoretical results also can be computed. A comparison of experimental and theoretical results is discussed in Section 4.

4. Results and Discussion

The measured TPF intensity profiles as a function of focal depth are shown in Fig. 2(a) for six different scattering parameters. In this experiment, the scattering coefficient of the media was changed by adding a different amount of polystyrene spheres of 0.304-μm diameter into the Rhodamine 590 tetrafluoroborate dye solution. The corresponding computed intensity profiles are shown in Fig. 2(b). The confocal parameter z_0 of the excitation Gaussian

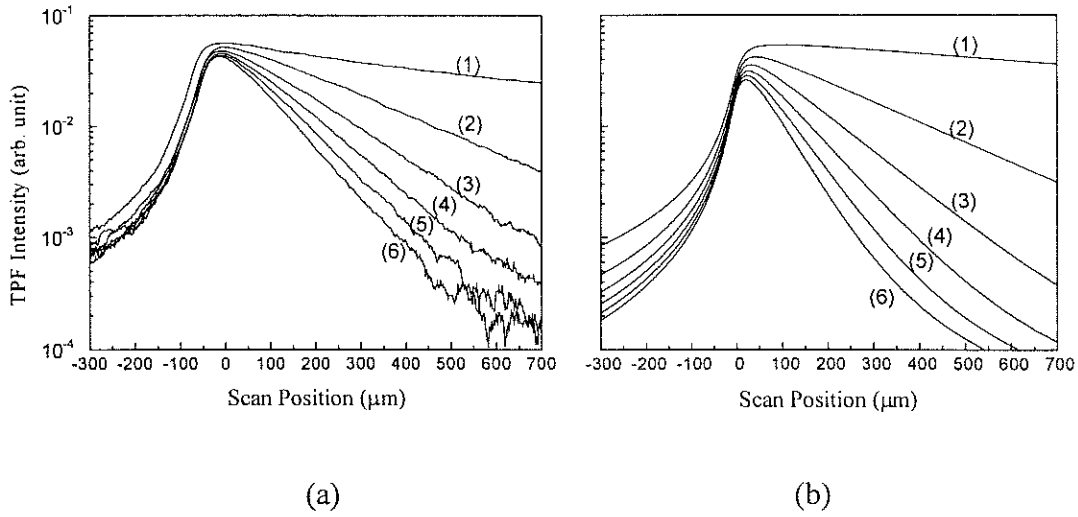

Fig. 2. (a) Measured TPF depth intensity profiles as a function of focal depth position for scattering media with a 0.304-μm-diameter polystyrene sphere. The scattering coefficients at 810 nm are (1), 0; (2), 0.78; (3), 1.57; (4), 2.32; (5), 3.07; and (6), 3.70 mm^{-1}. The scattering coefficient at 550-nm TPF emission is 2.68 times that at 810 nm. The volume concentrations of the polystyrene sphere scatterer are 0, 0.13%, 0.26%, 0.39%, 0.51%, and 0.63%. (b) Computed TPF depth intensity profiles when the scattering coefficients in Fig. 2(a) and Eq. (5) are used.

beam was determined to be 20 μm according to measurement of the axial TPF intensity profile of an ultrathin neat dye layer similar to that in Ref. 14. The diameter of the focal spot was estimated to be 4 μm with a method developed by Scheader *et al.*[14]

For curves (1)–(6) in Fig. 2(a), the scattering coefficients were 0, 0.78, 1.57, 2.32, 3.07, and 3.77 mm^{-1} at a 810-nm wavelength. The scattering coefficient at 550-nm TPF emission is 2.68 times that at 810 nm. These data were used to calculate the theoretical TPF profile by Eq. (5), as shown in Fig. 2(b). From Fig. 2(a) the salient feature of these intensity profiles shows that the nonlinear optical signal increases as the focal point moves from outside the sample surface into the medium. The parameter determining the rising profile is z_0. A tighter focus, or smaller z_0, will produce a sharper rising edge.[7,15] The maximum peak intensity is located within 50 μm of the surface.

Exponential decay behavior is seen as the focal point is moved further into the medium. With the increase in scattering strength, the TPF intensity decays faster. Figure 2(b) shows the theoretical results calculated form Eq. (5). We see from Fig. 2(b) that the experimental results agree well with the computed results. Owing to the approximation of ballistic transport for Green's function, $G_{em}(\mathbf{r}, \mathbf{r}')$ in

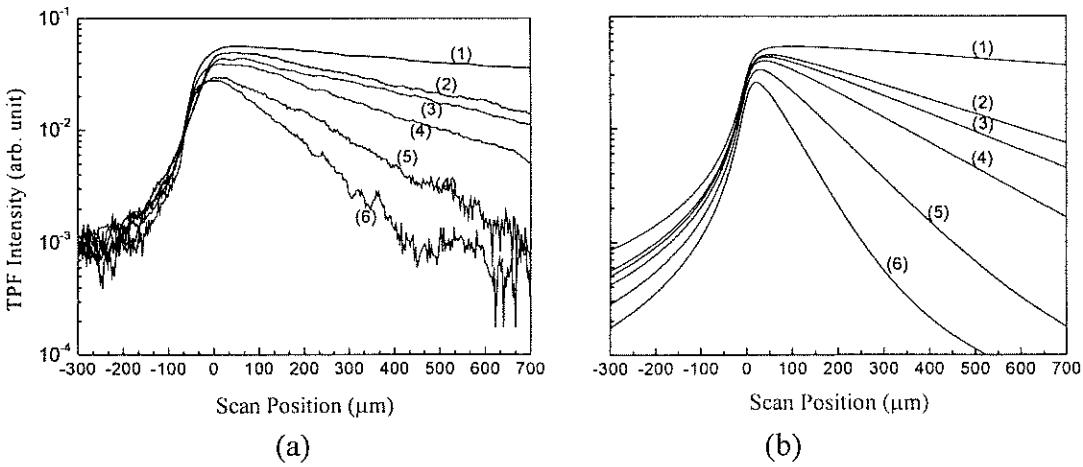

Fig. 3. (a) Measured TPF intensity depth profiles as a function of the focal depth position for scattering media with a 1.07-μm-diameter polystyrene sphere. The scattering coefficients at 810 nm are (1), 0; (2), 0.63; (3), 0.83; (4), 1.25; (5), 2.50; and (6), 5.00 mm^{-1}. The scattering coefficient at 550-nm TPF emission is 1.73 times that at 810 nm. The volume concentration of the polystyrene sphere scatterer is 0, 0.025%, 0.03%, 0.05%, 0.1%, and 0.2%. (b) Computed TPF depth intensity profiles when the scattering coefficients in Fig. 3(a) and Eq. (5) are used.

Eq. (4), there is a greater difference between the experimental and the theoretical results as the media become more scattering.

The measured TPF profiles for the second scattering media with the 1.07-μm-diameter polystyrene sphere are shown in Fig. 3(a). The scattering coefficients of the media are curve (1), 0; (2), 0.63; (3), 0.83; (4), 1.25; (5), 2.50; and (6) 5.00 mm^{-1}. The corresponding computed TPF profiles are shown in Fig. 3(b).

From Figs. 2 and 3 the TPF profile has an exponential decay. In Table 1 we compare the theoretical decay slope of the TPF profile with the experimentally measured slope for the two kinds of scattering media mentioned above. From Table 1 the deviation is greater for the larger scatterer (1.07 μm). The reason may be that for the larger 1.07-μm-diameter scatterer, light is scattered mostly in the forward direction (the larger g value). Thus the contribution from the diffusive component would be greater for the larger scatterer.

As shown in Table 1, the decay slope of the detected nonlinear optical signal is changed when the scattering strength of the medium is increased. For imaging the internal structure of scattering media, the degradation of the TPF intensity due to scattering is twofold. Scattering exponentially reduces the nonlinear optical intensity as the focal point is moved inside the medium. Scattering further reduces the reemitted TPF signal from the focal region. The signal-to-noise ratio of the detected nonlinear optical signal in turn is reduced.

For a more detailed comparison the difference percentage between the experimental $[I_{ex}(z_s)]$ and the theoretical $[I_{th}(z_s)]$ TPF intensity profiles are computed:

$$\Delta I(\%) = \frac{I_{ex}(z_s) - I_{th}(z_s)}{I_{ex}(z_s)} \times 100\%, \qquad (6)$$

where the peak of $I_{th}(z_s)$ is normalized to the experimental peak value. The results for the three different scattering strengths of each media are displayed in Fig. 4. For easy comparison the depth axis is normalized to the scattering MFP at the excitation wavelength. For a focus depth of 0.5 or more scattering MFP at the excitation wavelength, the experimental result differs from the theoretical model by 50%. The theoretical model overestimates the decrease of the TPF intensity as a function of focal depth. For a smaller scatterer the difference is smaller for the same optical depth. This indicates that there is a larger contribution from the diffusive component for the larger scatterer medium.

Because of the first-order approximation and ballistic transport model used in deriving Eq. (5), the diffusive component is not included, and the theoretical model overestimates the decay of the TPF intensity profile. Better predictive theoretical results could be obtained by including the diffuse light, which is beyond the scope of this paper.

The TPF spatial profile for a medium where a slice of glass 100 mm thick was inserted into the scattering media is shown in Fig. 5. The scattering coefficients for curves (1)–(4) are 0, 0.63, 0.83, 1.25 mm^{-1}. When the focal point of the laser beam was scanned along the z axis, a dip in the TPF

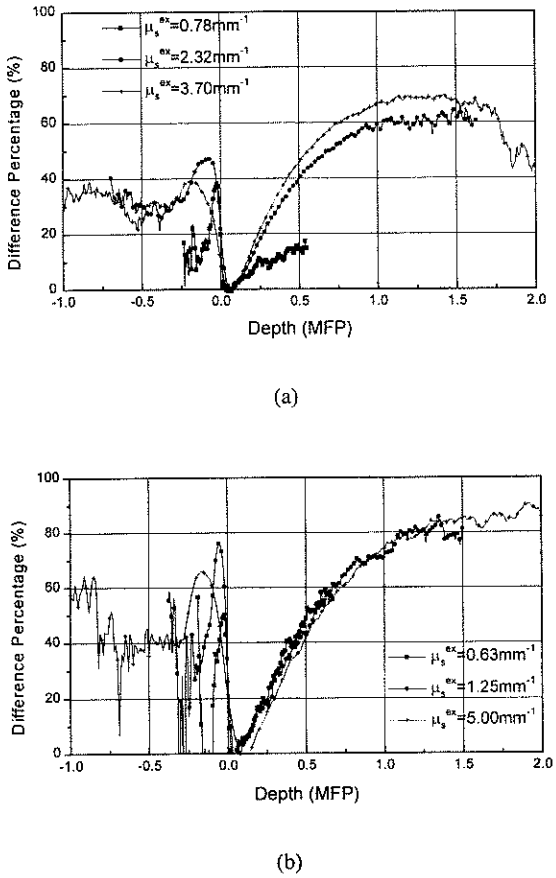

Fig. 4. Difference percentage between the experimental and the theoretical TPF intensity profiles for three different scattering strengths of each media with (a) 0.304- and (b) 1.07-μm-diameter polystyrene spheres.

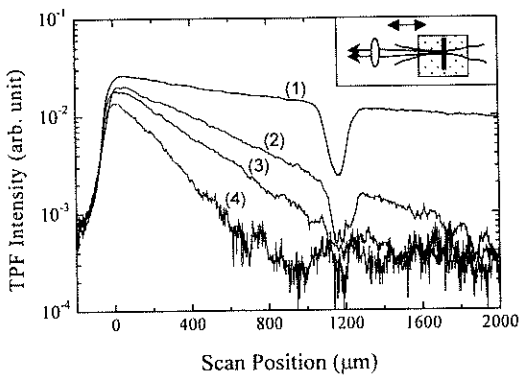

Fig. 5. TPF depth profile for a 1.07-μm sphere scattering medium with an inserted glass slice 100 μm thick for different scattering coefficients. The scattering coefficients are (1), 0; (2), 0.63; (3), 0.83; and (4) 1.25 mm^{-1}.

intensity profile appears at the position of the inserted slice of glass.

From the curves in Fig. 5 one can see that the ratio of signal to noise is decreased significantly as the scattering of media is increased. The appearance of the dip for the glass slice is difficult to see for the highly scattering medium [curve (4) in Fig. 5]. The important factor in the degradation is that the nonlinear optical (NLO) signal no longer comes from the focal region alone. On the contrary, the NLO signals generated near the sample surface contribute so significantly to the detected intensity that the optical depth sectioning ability of the microscopy is consequently degraded.[7] For biomedical applications the depth of direct imaging when the detected nonlinear optical intensity is used is limited to several scattering lengths or a few hundred micrometers. It is possible to use the detected nonlinear optical intensity profiles to reconstruct a 3-D map of the medium. A clearer image of the medium structure may be obtained with such a reconstruction.

5. Conclusions

In conclusion, the generation and detection of the NLO signal in highly scattering media has been studied by measuring TPF as a function of the focal depth from the uniform scattering media with different scattering strengths. The intensity of the TPF signal decays exponentially as a function of focal depth inside the medium. As the scattering strength of the medium increases, the intensity of the NLO signal decays more rapidly as the focal point is translated into the sample. Therefore the signal-to-noise ratio is decreased significantly when the scattering coefficient of the media is increased. The depth-sectioning ability of microscopy was decreased because the TPF signal was no longer confined to the focal region of a Gaussian beam. The experimental results are explained by taking into account the scattering loss of the excitation and the reemission of NLO light. The theoretical model overestimates the decay of TPF intensity because the diffusive components were excluded.

We thank B. Xu for help with the laser system and C. Nara for improving the manuscript. This research is supported in part by the U.S. Department of Energy Center of Excellence Program, the New York State Science and Technology Foundation, the NASA-Institutional Research Award, and the Air Force Office of Scientific Research.

References

1. W. Denk, J. H. Strickler, and W. W. Webb, "Two-photon laser scanning fluorescence microscopy," Science **248,** 73–76 (1990).
2. D. W. Piston, B. R. Masters, and W. W. Webb, "Three-dimensionally resolved NAD(P)H cellular metabolic redox imaging of the *in situ* cornea with two-photon excitation laser scanning microscopy," J. Microsc. **178,** 20–27 (1995).
3. S. Maiti, J. B. Shear, R. M. Williams, W. R. Zipfel, and W. W. Webb, "Measuring serotonin distribution in live cells with three-photon excitation," Science **275,** 530–532 (1997).
4. B. R. Master, P. T. C. So, and E. Gratton, "Multiphoton excitation fluorescence microscopy of *in vivo* human skin," Biophys. J. **72,** 2405–2412 (1997).
5. Y. Guo, P. P. Ho, H. Savage, D. Harris, P. Sacks, S. Schantz, F. Liu, and R. R. Alfano, "Second harmonic tomography of tissues," Opt. Lett. **22,** 1323–1325 (1997).
6. D. W. Piston, "Imaging living cells and tissues by two-photon excitation microscopy," Trends Cell Biol. **9,** 66–69 (1999).
7. J. Ying, F. Liu, and R. R. Alfano, "Spatial distribution of two-photon-excited fluorescence in scattering media," Appl. Opt. **38,** 224–229 (1999).
8. A. Diaspro and M. Robello, "Multiphoton excitation microscopy to study biosystems," Microsc. Anal. Americas Ed., Issue 35, 11–13 (March 1999).
9. R. R. Alfano and A. Katz, "Fluorescence and Raman spectroscopy for tissue diagnosis and characterization," in *Analytical Use of Fluorescent Probes in Oncology*, E. Kohen and J. G. Hirschberg, eds. (Plenum, New York, 1997), pp. 81–89.
10. W. F. Cheong, S. A. Prahl, and A. J. Welch, "A review of the optical properties of biological tissues," IEEE J. Quantum Electron. **26,** 2166–2185 (1990).
11. C. M. Blanca and C. Saloma, "Monte Carlo analysis of two-photon fluorescence imaging through a scattering medium," Appl. Opt. **37,** 8092–8102 (1998).
12. H. C. van de Hulst, *Light Scattering by Small Particles* (Dover, New York, 1981), Chap. 9.
13. B. E. A. Saleh and M. C. Teich, *Fundamentals of Photonics* (Wiley, New York, 1991), Chap. 3, pp. 80–92.
14. M. Schrader, U. G. Hofmann, and S. W. Hell, "Ultrathin fluorescent layers for monitoring the axial resolution in confocal and two-photon fluorescence microscopy," J. Microsc. **191,** 135–140 (1998).
15. S. Lindek, E. H. K. Stelzer, and S. W. Hell, "Two new high-resolution confocal fluorescence microscopes (4pi, theta) with one and two-photon excitation," in *Handbook of Biological Confocal Microscopy*, 2nd ed., J. B. Pawley, ed. (Plenum, New York, 1995), pp. 417–430.